Ultrafast laser structuring of high-voltage cathode materials for lithium-ion batteries

Carolyn Reinhold*, Wilhelm Pfleging

Karlsruhe Institute of Technology, Institute for Applied Materials – Applied Materials Physics (IAM-AWP), Hermann-von-Helmholtz-Platz 1, 76344 Eggenstein-Leopoldshafen, Germany

ABSTRACT

A rather new approach for simultaneously achieving high energy and high-power density of a battery electrode is the use of a high-voltage cathode material in conjunction with a three-dimensional (3D) electrode architecture created through ultrafast laser structuring. In the presented work, $LiNi_{0.5}Mn_{1.5}O_4$ (LNMO) cathodes were laser structured using a high-power ultrashort pulsed laser source with an average laser power up to 300 W. An investigation of the ablation behavior of LNMO cathodes was performed by a variation of laser and process parameters. The impact of the laser pulse peak fluence and the repetition rate on the ablation depth and width of the generated grooves was analyzed, while keeping the pulse-to-pulse distance constant. An electrochemical analysis of unstructured and selected laser structured LNMO cathodes was conducted to study the influence of the laser structuring on the electrochemical performance. It could be shown that the combination of LNMO with the advantages of a 3D electrode design is leading to outstanding electrochemical properties.

Keywords: Ultrashort pulsed laser ablation, lithium-ion battery, 3D battery, laser structuring, LNMO

1. INTRODUCTION

The electrification of transportation presents a challenge in the need for batteries that can provide simultaneously high energy and power density, while being safe in operation and sustainable as well as cost-effective in production. For achieving this purpose, both material and electrode architecture must be further developed.

Concerning the material, high energy densities can be achieved by using electrode materials providing high specific capacities and working potentials. Popular cathode material candidates for use in battery electric vehicles are lithium nickel manganese cobalt oxides $Li(Ni_xMn_yCo_{1-x-y})O_2$ (NMC). By increasing their nickel content practical specific capacities up to 190 mAh g^{-1} (NMC811) can be reached [1]. This allows, according to Armand et al [1], by combining such a cathode with a graphite anode to reach an energy density up to 448 Wh kg^{-1} on cell level.

Another interesting cathode material, which allows to realize even higher energy densities of 464 Wh kg^{-1} on cell level, is the high-voltage spinel $LiNi_{0.5}Mn_{1.5}O_4$ (LNMO) [1]. Main reason for this is the high working potential of 4.7 V which is 1 V higher than the one of NMC and therefore overcompensates the slightly lower practical specific capacity of 140 mAh g^{-1} [1, 2]. Further advantages, compared to NMC, are that LNMO is cobalt free and the redox capacity of nickel can be completely used [2]. In addition, its spinel structure enables fast Li^+ solid state diffusion over a three-dimensional network, providing high rate capability [3].

Concerning the electrode architecture, a high energy density can be reached using electrodes with a high mass loading. However, due to the high electrode thickness, the lithium diffusion kinetics of such electrodes are strongly limited leading to an increased cell polarization and in consequence to low power densities. A solution to overcome this problem is to implement a 3D electrode architecture by locally remove electrode material by laser ablation. The additional created electrode/electrolyte surfaces facilitate the Li^+-diffusion inside the electrolyte filled porous electrode structure leading to an overall reduced cell polarization. This results, especially at elevated C-rates, in enhanced rate capabilities during charge and discharge. [4, 5]

In previous works, the application of such a 3D electrode design and its positive impact on the electrochemical performance has already been demonstrated for different kind of cathode and anode active materials, including $LiFePO_4$ (LFP) [6], NMC [7], graphite [8], and silicon/graphite [9]. Aim of the ongoing research is to merge the concept of the 3D

electrode design with the use of a high-voltage cathode material and to upscale the technology with respect to battery and module fabrication [10].

In the presented approach, LNMO cathodes are laser structured using a high-power ultrashort pulsed laser source. An investigation of the ablation characteristics of LNMO cathodes is performed by a variation of laser and process parameters. The influence of the repetition rate and the pulse peak fluence on the resulting ablation depth and structure width is analyzed and discussed. Finally, the electrochemical properties of cells containing selected laser structured and unstructured LNMO cathodes are evaluated using rate capability measurements.

2. EXPERIMENTAL

2.1 Electrode manufacturing

The LNMO cathodes were manufactured via the following procedure. Prior to the slurry mixing, an N-methyl-2-pyrrolidone-based (NMP, Merck, Germany) PVDF (Solvay, Germany) solution with a weight ratio of 1:10 is prepared by using a SpeedMixer (DAC 150 SP, Hauschild, Germany). For the slurry production, LNMO powder (Haldor Topsoe, Denmark) and conductive carbon black (CB, C-NERGY C65, Imerys G&C, Belgium) were manually mixed, before adding to the PVDF solution. Further NMP solution was added to the mixture to adjust the slurry viscosity and the solid content. The mixing of the electrode slurry was performed in the same SpeedMixer as the preparation of the PVDF solution.

The electrode slurry was deposited on an aluminum current collector foil (20 µm thickness) with a universal applicator (ZUA 2000, Proceq, Switzerland) on a film coater (MSK-AFA-III, MTI Corporation, USA) and dried at 90 °C for two hours. The final composition of the LNMO cathode is shown in Table 1. Afterwards, the LNMO cathodes were calendered to adjust a porosity of 35 % using an electric rolling presser (MSK-2150, MTI, Cooperation, USA).

Table 1. Composition of the LNMO cathodes.

Material	Mass fraction / wt.%
LNMO	93
C65	4
PVDF	3

2.2 Laser structuring

For the ablation study of the LNMO cathodes a laser material processing system (MSV203 Laser Patterning Tool, M-Solv LTD, United Kingdom) equipped with a high-power, high repetition rate laser source (FX600-2-GFH, EdgeWave GmbH, Germany) operating at a wavelength of 1030 nm, a pulse length of 600 fs and a maximum average power (P_{avg}) of 300 W was used. A schematic illustration of the setup of the whole system can be seen in Figure 1. At the exit of the laser source, the raw beam has a radius of 1295 µm in x-direction and 1373 µm in y-direction (M^2_x = 1.11; M^2_y = 1.07) which is magnified by the factor of 6 through a beam expander telescope. With the aid of a beam splitter, the laser beam is split into two separate beams which are each directed to a scanner (IntelliScan III 20, SCANLAB GmbH, Germany) and a F-theta lens (JENar, JENOPTIK AG, Germany) with a focal length of 255 mm. The focused beam has then a calculated beam radius of 11.95 µm in x-direction and 10.85 µm in y-direction.

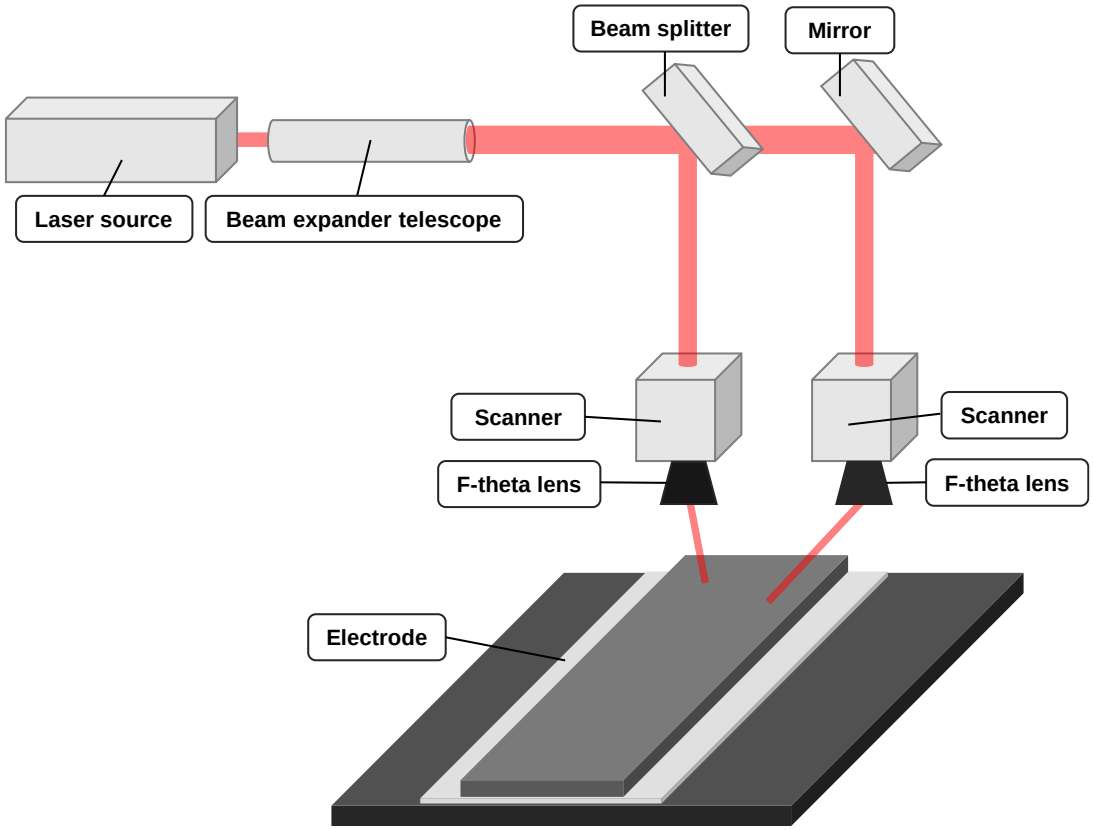

Figure 1. Schematic drawing of the setup of the used laser material processing system.

The investigation of the ablation behavior of the LNMO cathodes was conducted with a constant pulse-to-pulse distance of 13.3 µm which allows the realization of line patterns. The applied repetition rates f and corresponding scan speeds v can be found in Table 2. In addition, the ratio of the average laser power P_{avg} to the repetition rate f was kept constant, so that the influence of the repetition rate f with a constant pulse peak fluence E_p on the ablation behavior can be analyzed. Depending on the repetition rate, average laser powers between 1 W and 100 W were applied, leading to pulse peak fluences between 3 J cm^{-2} and 33 J cm^{-2}. The number of repetitions was varied between 3 and 15. For each set of parameters, several lines were created. The ablation depth as well as the ablation width at the top of the created grooves were measured using a digital microscope (VHX 7000, Keyence, Japan).

Table 2. Applied repetition rate and scan speed corresponding to a pulse-to-pulse distance of 13.3 µm.

Repetition rate / kHz	Scan speed / m s^{-1}
150	2
750	10
1500	20

2.3 Electrochemical testing

For an analysis of the electrochemical performance, unstructured as well as structured LNMO cathodes generated with the parameter set corresponding to the highest aspect ratio were cut in circles with a diameter of 12 mm and dried at 110 °C in a vacuum oven (VT6025, Thermo Scientific, Germany) for 16 hours. The LNMO cathodes were afterwards assembled in CR2032 coin cells versus lithium (0.6 mm thickness, Nanografi, Turkey) in an argon-filled glovebox (LABmaster pro,

M.Braun, Germany) with H_20 < 0.1 ppm and O_2 < 0.1 ppm. As separator between the LNMO cathode and the lithium metal a 20 µm trilayer microporous membrane (polypropylene/polyethylene/ polypropylene) (Celgard® 2320, USA) was used. A total amount of 120 µl electrolyte was added, consisting of 1.3M hexafluorophosphate ($LiPF_6$) dissolved in a mixture of ethylene carbonate (EC) and ethyl methyl carbonate (EMC) with a weight ratio of 3:7 and 5 wt.% fluoroethylene carbonate (FEC). The sealing of the cells was conducted using an electric cell crimper (MSK-160D, MTI Corporation, USA). For the formation and the subsequent rate capability measurements of the cells, a constant current – constant voltage (CCCV) protocol for charging and a constant current protocol for discharging was applied by using a battery cycling system (BT 2000, Arbin Instruments, USA). The C-rates (i.e., applied electrical current divided by nominal cell capacity) for the different steps can be taken from Table 3. The voltage window for all steps was set to 3.5 V to 4.9 V.

Table 3. C-rates applied for the formation and the rate capability measurement steps.

C-rate for CC charge / h^{-1}	0.05	0.1	0.2	0.5	0.5	0.5	0.5	0.5	0.5
C-rate for CV charge / h^{-1}	0.02	0.05	0.05	0.05	0.05	0.05	0.05	0.05	0.05
C-rate for CC discharge / h^{-1}	0.05	0.1	0.2	0.5	1	2	3	5	0.2
Number of cycles	3	5	5	5	5	5	5	5	5

3. RESULTS AND DISCUSSION

3.1 Investigation of the ablation behavior

The ablation behavior of the LNMO cathodes was studied by keeping the same ratio of scan speed v and repetition rate f for all applied repetition rates. Furthermore, the ratio of the average laser power P_{avg} to the repetition rate f was kept constant to investigate the influence of the repetition rate with a constant pulse peak fluence. In Figure 2, the ablation depth and ablation width at the top of the grooves for the LNMO cathodes are shown as a function of the pulse peak fluence for the different applied repetition rates. For all repetition rates, increasing the pulse peak fluence increases the ablation depth as well as the ablation width.

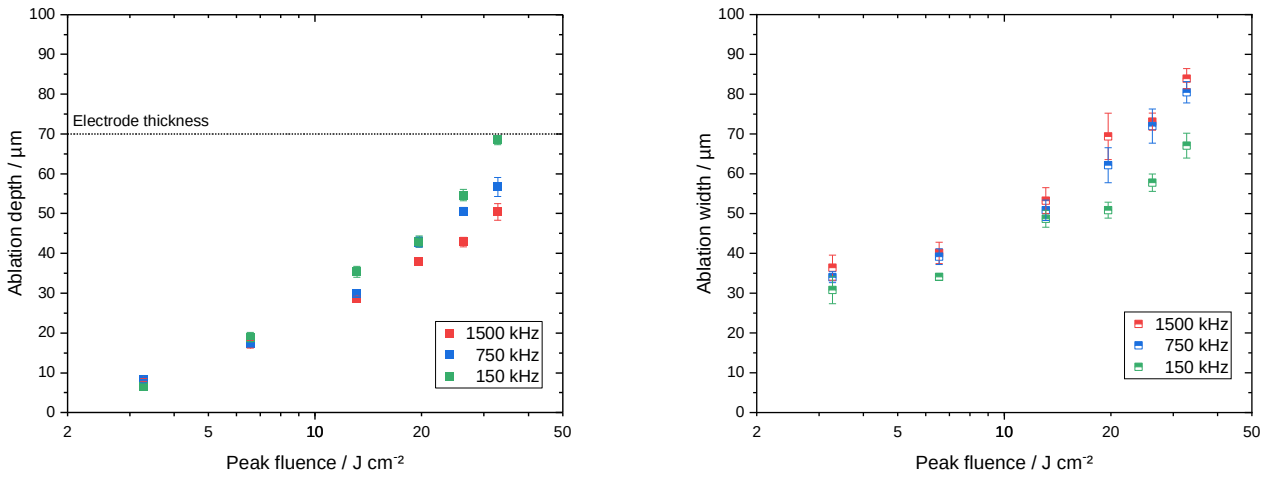

Figure 2. Ablation depth (left) and width (right) depending on the pulse peak fluence E_p for LNMO cathodes for different repetition rates. (n =9).

However, it is noticeable that the lower the repetition rate, the higher the ablation depth and the lower the ablation width for equal pulse peak fluences. For example, at a pulse peak fluence of 33 J cm^{-2} an ablation depth of 69 µm for a repetition rate of 150 kHz was achieved, which is equal with the electrode thickness, whereas an ablation depth of 50 µm for a repetition rate of 1500 kHz could be reached. In accordance, the ablation width increased from 67 µm at a repetition rate of 150 kHz to 84 µm at a repetition rate of 1500 kHz. Responsible for this finding might be shielding effects by the laser-induced vapor/plasma plumes. At high repetition rates, the laser pulse can interact with the generated vapor/plasma plume of the previous pulse leading to an attenuation of the incident beam and in consequence to a decrease of ablated electrode material. Therefore, to achieve generated grooves with a high aspect ratio, meaning a low mass loss, lower repetition rates should be preferred.

The findings are in accordance with other works, where comparable results can be found for other electrode materials such as graphite and silicon/graphite with a CMC-SBR binder system [9, 11]. This shows that the ablation of the electrode material is based on the same principle, independent of the active material and the binder that is used. The scanning electron microscope images in Figure 3 show that by laser structuring the investigated LNMO cathode at a repetition rate of 150 kHz with a pulse peak fluence of 33 J cm^{-2} and nine repetitions the complete material of the composite electrode can be removed in the laser beam interaction area. The aluminum current collector seems not to be modified and no debris formation or re-deposition of particles on the remaining composite electrode can be detected. The active material particles seem not to be affected by the ultrafast laser ablation indicating that the binder decomposition and subsequent ejection of LMNO particles is the dominating ablation mechanism quite similar to the thermally driven ablation of composite electrodes as described by Pfleging et al. [12]. However, in contrast to thermally driven ablation no decomposition or melt formation of active material occurs.

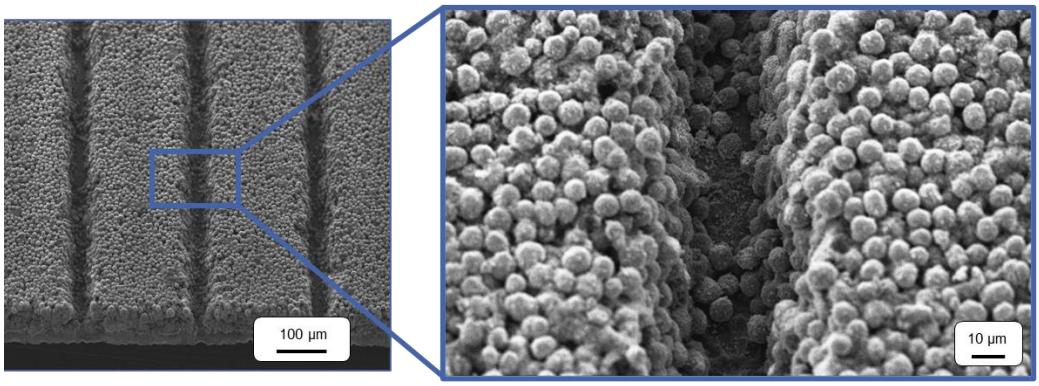

Figure 3. Scanning electron microscope images of a structured LNMO cathode (f = 150 kHz, E_p = 33 J cm^{-2}, n = 9).

3.2 Electrochemical testing

Rate capability measurements on unstructured and structured LNMO cathodes were conducted to analyze the effect of the laser structuring on the electrochemical performance. Figure 4 shows the specific discharge capacities of the cells containing the unstructured and structured LNMO cathodes depending on the different applied C-rates. At low C-rates (C/20 till C/2), for both types of electrodes, a specific discharge capacity between 135 mAh g^{-1} and 137 mAh g^{-1} can be achieved. By increasing the C-rate to higher values (1C till 5C), the specific discharge capacity decreases with increasing C-rate. However, the capacity decrease can be reduced for the cells containing the laser structured LNMO cathodes, especially at C-rates of 3C and 5C. For example, an average specific discharge capacity of 99 mAh g^{-1} can still be achieved at 5C for the cells with the structured LNMO cathodes, whereas the cells with the unstructured LNMO cathodes are only able to reach 35 mAh g^{-1}. This corresponds to a capacity increase of around 280 % in case of using laser structured LNMO cathodes instead of unstructured ones.

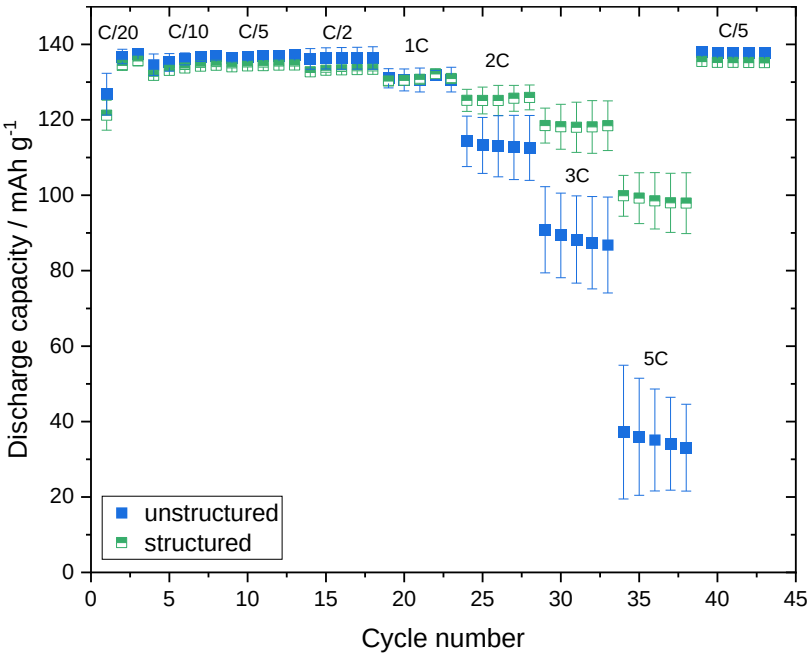

Figure 4. Rate capability measurements of cells containing unstructured and structured LNMO cathodes.

The increase of the discharge capacity for cells containing structured electrodes can mainly be associated with the improved Li^+ diffusion kinetics. Due to the laser structuring, new contact surfaces between the porous electrode structure and the electrolyte are generated shortening the Li^+ diffusion pathways inside the porous electrode. Consequently, the Li^+ concentration gradient and thus the overpotential are reduced, resulting in elevated specific discharge capacities even at higher C-rates.

4. CONCLUSION

LNMO cathodes were manufactured using an NMP-based electrode processing. The electrodes were afterwards laser structured using a high-power ultrashort pulsed laser source. An investigation of the ablation behavior was performed by varying the repetition rate and pulse peak fluence while keeping a constant pulse-to-pulse distance. It could be shown that both the ablation depth and the ablation width have a dependency on the applied repetition rate and pulse peak fluence. For all pulse peak fluences, increasing the repetition rate leads to lower values for the ablation depth and higher values for the ablation width. An analysis of the electrochemical performance for unstructured and selected laser structured LNMO cathodes was conducted in coin cells versus lithium. Rate capability measurements showed, especially at high C-rate like 2C, 3C and 5C, an increase of the specific discharge capacity for laser structured LNMO electrodes in comparison to unstructured ones. For example, for a C-rate of 5C, the specific discharge capacity could be increased from 35 mAh g^{-1} to 99 mAh g^{-1} due to laser structuring, which corresponds to a capacity increase of around 280 %.

ACKNOWLEDGEMENT

This project receives funding from the European Union's Horizon Europe research and innovation program under grant agreement no. 101069508 (HighSpin).

REFERENCES

[1] Armand, M. et al. 2020. Lithium-ion batteries – Current state of the art and anticipated developments. *Journal of Power Sources*. doi: 10.1016/j.jpowsour.2020.228708.

[2] Stüble, P. et al. 2023. On the Composition of $LiNi_{0.5}Mn_{1.5}O_4$ Cathode Active Materials. *Advanced Energy Materials*. doi: 10.1002/aenm.202203778.

[3] Fehse, M. et al. 2022. Influence of Transition-Metal Order on the Reaction Mechanism of LNMO Cathode Spinel: An Operando X-ray Absorption Spectroscopy Study. *Chemistry of materials: a publication of the American Chemical Society*. doi: 10.1021/acs.chemmater.2c01360.

[4] Pfleging, W. 2021. Recent progress in laser texturing of battery materials: a review of tuning electrochemical performances, related material development, and prospects for large-scale manufacturing. *International Journal of Extreme Manufacturing*. doi: 10.1088/2631-7990/abca84.

[5] Pfleging, W. 2022 - 2022. 3D electrode architectures for high energy and high power lithium-ion batteries. In: Balaya, P. et al. [Hrsg.] *Energy Harvesting and Storage: Materials, Devices, and Applications XII.* SPIE. 2.

[6] Mangang, M. et al. 2014. Ultrafast laser microstructuring of $LiFePO_4$ cathode material. In: Klotzbach, U. et al. [Hrsg.] *Laser-based Micro- and Nanoprocessing VIII.* SPIE. 89680M.

[7] Song, Z. et al. 2021. Electrochemical Performance of Thick-Film $Li(Ni_{0.6}Mn_{0.2}Co_{0.2})O_2$ Cathode with Hierarchic Structures and Laser Ablation. *Nanomaterials*. doi: 10.3390/nano11112962.

[8] Jan Bernd Habedank. 2021. *Laser Structuring of Graphite Anodes for Functionally Enhanced Lithium-Ion Batteries.* Dissertation. München.

[9] Meyer, A. et al. 2023. High repetition ultrafast laser ablation of graphite and silicon/graphite composite electrodes for lithium-ion batteries. *Journal of Laser Applications*. doi: 10.2351/7.0001180.

[10] Sterzl, Y. und Pfleging, W. Extending the 3D-battery concept: large areal ultrashort pulsed laser structuring of multilayered electrode coatings. In: 29.

[11] Pfleging, W. et al. 2014. Laser generated microstructures in tape cast electrodes for rapid electrolyte wetting: new technical approach for cost efficient battery manufacturing. *Proceedings of SPIE - The International Society for Optical Engineering*. doi: 10.1117/12.2039635.